Conf-740637--2

ELASTIC AND INELASTIC HEAVY ION SCATTERING*

G. R. Satchler
Oak Ridge National Laboratory
Oak Ridge, Tennessee

1. Introduction

Despite my title, I shall say very little about inelastic scattering. It can be used, of course, in the standard spectroscopic way to extract reduced transition probabilities. Further, by studying the interference between the nuclear and Coulomb excitation contributions, important things can be learnt about the former; Broglia will talk about that.

I think we all know that heavy ion interactions are dominated by the fact of strong absorption and that to a considerable degree they can be understood in semi-classical and simple optical terms. Rather than attempt a review of these things (several good reviews are already available; see, for example, [1,2] and references given there), I will attenpt to discuss some specific points of what we may hope to learn from elastic scattering studies. It seems to me to be important to know about these "entrance" conditions before we evaluate other, more complicated, processes that may occur when two ions collide. These conditions are revealed to us not only through elastic scattering but through other peripheral processes such as inelastic scattering and one or more nucleon transfer reactions. These various processes may, and usually do, probe different regions of the ion-ion interaction and it is important to consider them all together in order to get a full picture [3,4].

2. General Properties

The collision process may be divided into three spatial regions:

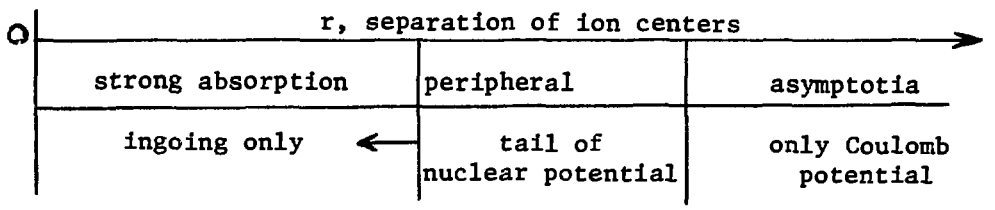

The outer region is of no interest. We are not likely to be able to describe the inner region in detail, but fortunately it seems that all we need to know is that it is essentially "black". The interesting peripheral region, where the ion surfaces interact, may be quite narrow (2 fm) and allows us to define nuclear radii or, better, interaction radii [1,2,5,6]. This is obvious from the data when cross sections are plotted against the distance of closest approach, D, of the corresponding classical (Rutherford) orbit. Figure 1 presents a nice example [7]. The cross sections remain close to Rutherford until a fairly well defined value of $D = D_o$ is reached, then decrease exponentially as absorption sets in. Further, this value is almost independent of energy and varies with the ion masses like

*Research sponsored by the U. S. Atomic Energy Commission under contract with Union Carbide Corporation.

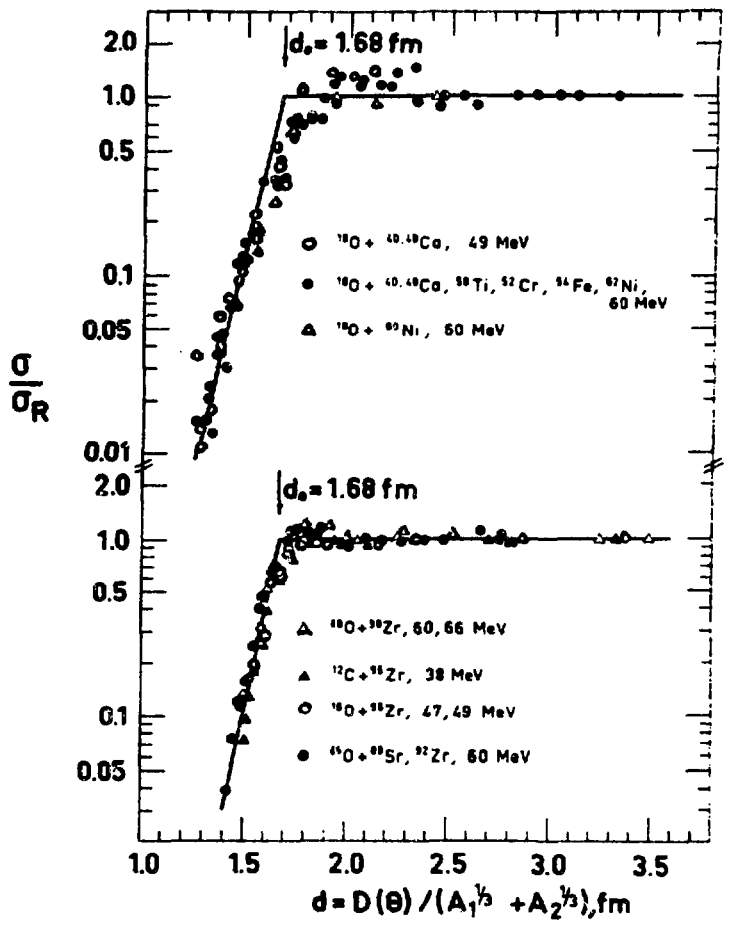

Figure 1

$(A_1^{1/3}+A_2^{1/3})$. D_o roughly corresponds to the outer limit of the peripheral region above. The falloff allows one to define an absorption probability for the region $D < D_o$,

$$P_{abs} = 1 - \exp((D-D_o)/\Delta),$$

with $\Delta \approx 0.55$ fm.

To go further, let me remind you of some definitions. The scattering cross section for two spinless ions (or where spin effects can be neglected) is $d\sigma/d\omega = |f(\theta)|^2$, where the scattering amplitude consists of a Coulomb and a "nuclear" part,

$$f(\theta) = f_c(\theta) + \frac{i}{2k}\sum_L (2L+1)\, e^{2i\sigma_L}\,(1-\eta_L)\, P_L(\cos\theta), \qquad (1)$$

where η_L is the partial wave scattering amplitude. The so-called transmission coefficient is $T_L = 1 - |\eta_L|^2$. In the strong absorption situation, the dependence on L is [1]:

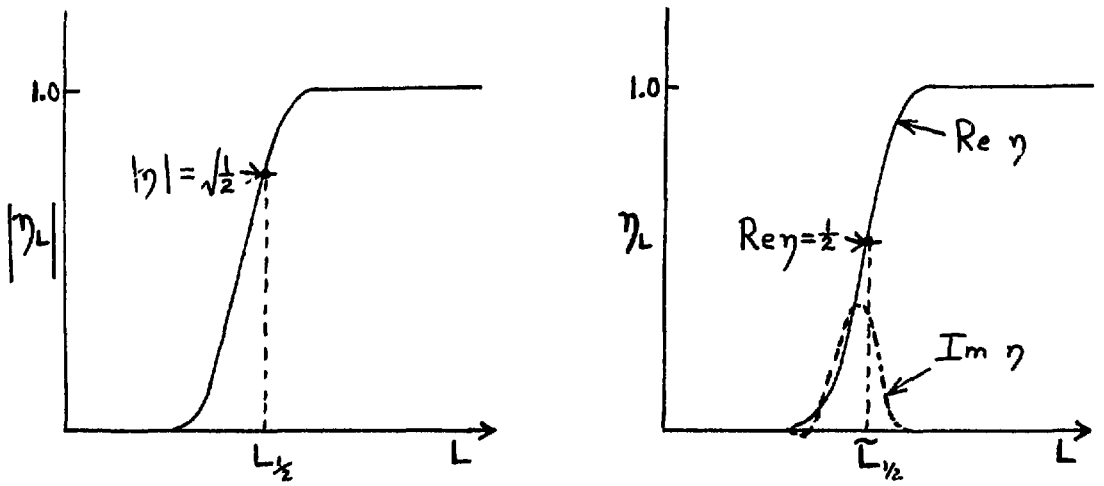

Figure 2

A critical $L_{1/2}$ is defined for which $T_L = 1/2$ (some people prefer to define $\tilde{L}_{1/2}$ for which $\mathrm{Re}\eta_L = 1/2$; $\tilde{L}_{1/2}$ is usually about one unit less than $L_{1/2}$). Through the classical (Rutherford) orbit relations,

$$L = n \cot(\theta/2) \quad , \quad D = (n/k)(1 + \sqrt{1 + (L/n)^2}), \tag{2}$$

where n is the usual Coulomb parameter and k is the wave number, we can obtain the corresponding critical scattering angle $\theta_{1/2}$ and distance of closest approach, $D_{1/2}$, for the orbit with $L = L_{1/2}$.

When the scattering is Coulomb dominated (as it usually is, except for the lightest targets or for very high energies), the angular distribution has the form of fig. 3, characteristic of Fresnel diffraction [2]. This suggests another critical angle, $\theta_{1/4}$, at which $d\sigma/d\sigma_R = 1/4$, and the corresponding $L_{1/4}$ and $D_{1/4}$. It turns out that $D_{1/4} \simeq D_{1/2}$, $L_{1/4} \simeq L_{1/2}$. Approximately, the data show that

$$D_{1/2} \approx 1.5(A_1^{1/3}+A_2^{1/3}),$$

which is of the order of 1 fm smaller than the radius (fig. 1) at which absorption begins to set in. Further, it is of the order of 2-3 fm larger than the sum of the radii of the two ions at which their densities reach 1/2 the central value. This situation is further illustrated in fig. 4 for the example of 72 MeV ^{16}O on ^{28}Si. The full circles have the half-density radii, the dotted circles show where the density is 10% of the central value and the separation of their centers represents the classical distance of closest approach at that L. Even when the absorption is almost complete, only the low ($\lesssim$ 10%) density regions of the two ions overlap (classically). (Remember that "absorption" means removal from the entrance or elastic channel into some non-elastic channel.) We return to fig. 4 later.

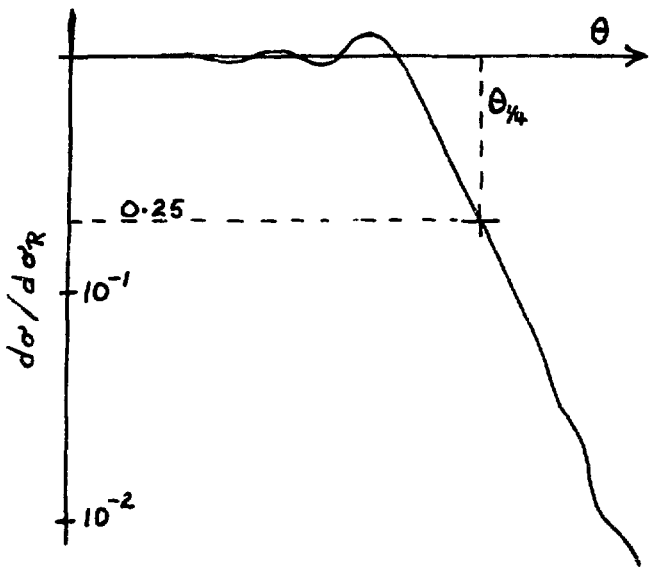

Figure 3

The almost universal behaviour of η_L with L (figs. 2, 4) has led to the (very successful) use of parametrized functional forms for $\eta(L)$ [1,6] which thereby incorporate gross physical information like strong absorption, nuclear size and surface thickness. However, it is possible that one's guesses for the form of $\eta(L)$ may overlook or obscure (or even violate) some physical implications which a more dynamic approach might include. These analyses have been reviewed in detail elsewhere [1,6].

The parametrized form of $\eta(L)$ has been generalized in the spirit of postulating Regge poles, which can introduce kinks into the smooth curve [8]. This still remains a parameterization, albeit perhaps a useful and suggestive one.

3. The Optical Model

The main alternative to these descriptions is given by the optical model which postulates a complex ion-ion potential which, usually, depends only upon

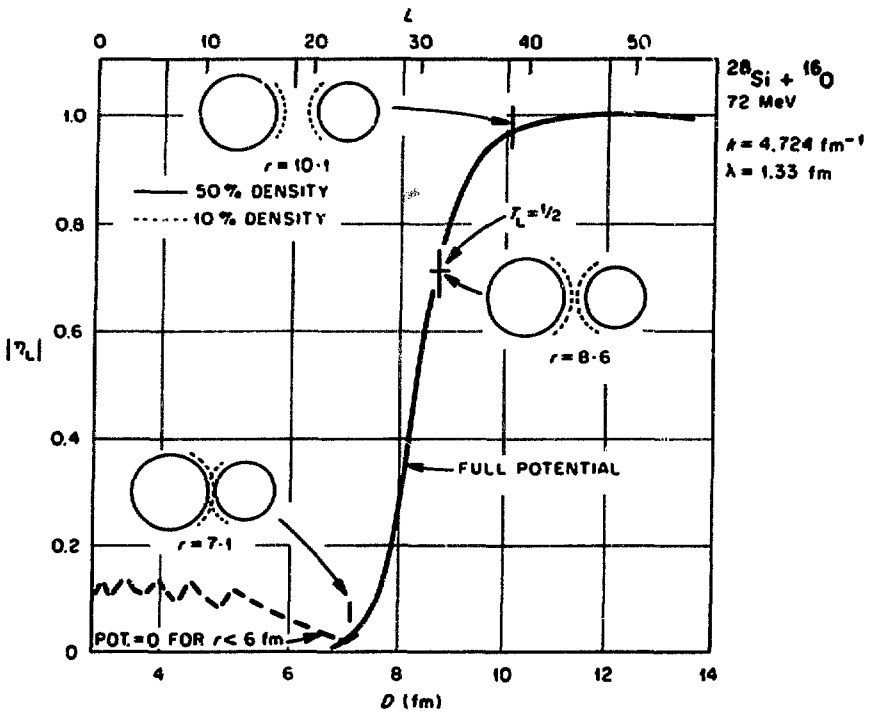

Figure 4

the separation of the centers of mass of the two, undisturbed, ions. (An exception occurs when the generalized model is used which includes coupling to inelastic channels and requires solution of a set of coupled equations. Of course, it is the coupling to other channels which gives rise to the imaginary part of the optical potential. Coupling to one specific channel may become important, in the sense that its effects cannot be represented by a simple absorptive potential, when the cross section for that channel becomes comparable to the elastic cross section. I don't have any statistics on that, but I think it is most likely to occur for inelastic scattering to a strong collective state.)

Traditionally this kind of optical potential has met with considerable scepticism, because clearly it has no direct meaning in the strong absorption region where the two ions overlap. Fortunately, however, this usually does not matter; the important region is the peripheral one where the two densities overlap very little and there is good reason to believe that a simple potential concept could be meaningful. A further advantage of the optical potential model is that it enables us to generate wavefunctions throughout all space, which the parametrized phase shift models cannot do. These wavefunctions can then be used in other reaction calculations (e.g. the DWBA). Again one treats these wavefunctions with considerable reservation in the strong absorption region, but again it is the peripheral region which is important and within which there is some hope that the wavefunctions are meaningful. (An alternative procedure which perhaps does less violence to one's physical prejudices is to define the potential only in the peripheral region; at the entrance to the strong absorption we simply impose an ingoing-wave boundary condition [9]. This black-hole model has not been exploited very much; it may have some computational advantages when high angular momenta are involved.)

Various attempts have been made to calculate the real parts of ion-ion potentials (usually for the $^{16}O+^{16}O$ system) [10]; sometimes these lead to strongly repulsive potentials when the ions overlap (sudden approximation), sometimes to weakly attractive ones (adiabatic limit). Sometimes, too, these approaches introqualitatively new features into the optical model, such as an explicit dependence of the mass parameters on the distance between the two nuclei [11]. A common feature of these calculations is that asymptotically the potential goes over to the "folded" form I shall discuss later. Attempts have also been made to calculate the imaginary, absorptive, potential [12].

It is worth mentioning at this point that the optical model is a very

general concept; indeed it is not unique, except insofar as it is defined to generate the same wavefunction beyond the region of interaction (i.e. the same elastic scattering) as the true many-body problem. There are various ways of extrapolating into the interior and the associated wavefunctions will have different meanings. This possibility must be kept in mind when the wavefunctions are used for other purposes, such as in a DWBA calculation of some reaction. For example, the wavefunction resulting from the potential given by, say, a two-center shell model calculation is really a different object in general from that given by the usual phenomenological optical potentials.

The optical models used in practice obey another constraint that they must be simple enough to be useful. The conventional form used for the phenomenological optical potential is the local Woods-Saxon (WS) one,

$$U(r) = -V(e^{x}+1)^{-1} - i\,W(e^{x'}+1)^{-1}, \qquad (3)$$

where $x = (r-R)/a$, $x' = (r-R')/a'$. For convenience, the radii are usually parametrized like $R = r_o(A_1^{1/3}+A_2^{1/3})$. Most often the four-parameter form, $R = R'$ and $a = a'$, is used. (There does seem to be evidence [13] that the potentials for ^{6,7}Li scattering require r_o' appreciably larger than r_o. This is reminiscent of the behaviour of deuterons and ^{3}He; in that case it is attributed to the easy breakup of the weakly bound projectile.) Of course, all the parameters can be expected in general to depend upon the bombarding energy and, as has been emphasized recently [12,14], upon the angular momentum. The latter dependence usually has only been considered for the absorptive strength, $W = W(L)$. If the ions' wavelength is sufficiently small so that the orbits can be fairly well localized, an effective L-dependence of the absorption can be induced by reducing ImU(r) in the surface region (e.g. by making R' and/or a' smaller than the corresponding R or a). It is not clear to me at this moment whether one can then distinguish between these two prescriptions, or indeed whether there is much physical difference between them.

4. Ambiguities and ^{11}B+^{208}Pb

A well-known feature of optical model fitting to elastic data for strongly-absorbed particles is the tremendous ambiguity; many sets, and often continuous distributions, of parameters will give equally good fits [1]. The most familiar of these is known as the Igo ambiguity and occurs because the scattering is mostly determined by the tail of the real potential [15]. At large radii,

$$\text{Re } U(r) \approx -(V \exp(R/a))\exp(-r/a),$$

so for a fixed value of a, any pair of V, R which keep $V\exp(R/a)$ constant will give the same tail even though the potentials in the interior may be very different.

However, the data do not necessarily determine the value of a, and hence the shape of the tail, at least in the cases I have looked at. Rather, what is determined is the value of the real potential at the critical radius $r = D_{1/2}$ discussed above. As an example, fig. 5 shows typical fits to cross sections for ^{11}B on ^{208}Pb [16] with 4, 5 or 6 parameter potentials, with real depths ranging from 20 to 200 MeV and with imaginary strengths $W/V \simeq 0.1$ to 0.4. The "best" fit (i.e. minimum χ^2) obtained is that shown on the right. The theoretical curve manages to reproduce the two data near 50°; the wiggles are real and not the result of numerical inaccuracy. This case is an example of the dangers of pushing for minimum χ^2 when only limited data are available; it turns out that this potential is quite unacceptable when used in calculations of inelastic scattering or transfer

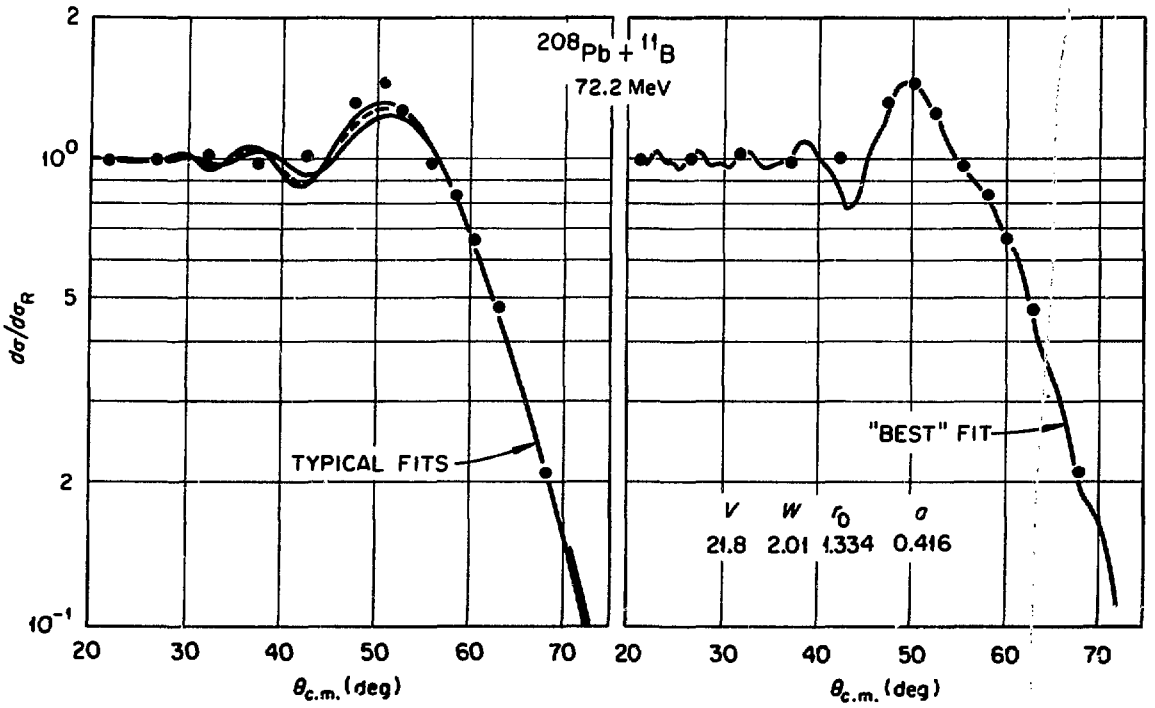

Figure 5

reactions [17]. (This example therefore also stresses the value of considering these other kinds of data as well as elastic scattering.) Figure 6 shows some of the corresponding real potentials (including the unacceptable one) at large radii. Clearly the one unambiguous thing these data tell us is the value of the potential near 12.15 fm (the critical distance in this case is $D_{1/2} = 12.0$ fm, for $L_{1/2}$ between 37 and 38), whereas the slope can vary widely. (The imaginary potential is also poorly determined.)

In passing we might note that this value of the potential is very small compared to the Coulomb barrier in that region which is about 50 MeV. Indeed this is almost invariably the case; if we take a "typical" nuclear optical potential [6] and evaluate it for $r = D_{1/2} \approx 1.5(A_1^{1/3}+A_2^{1/3})$, we get $U_N \approx -40 \exp[-0.4(A_1^{1/3}+A_2^{1/3})]$ MeV while the Coulomb potential is $U_C \approx Z_1Z_2(A_1^{1/3}+A^{1/3})^{-1}$ MeV. Even for $^{16}O+^{16}O$, U_N is less than half U_C, while the ratio U_N/U_C decreases rapidly as the charges on projectile and/or target increase. For example, for $^{16}O+^{208}Pb$, U_N is only 2% of U_C at this radius.

5. Folding Models

At these large radii the two ion densities scarcely overlap at all (figs. 4 and 7) and this suggests an approximation [2,17] in which the densities are assumed to be unperturbed and the real optical potential is simply the expectation value of a nucleon-nucleon interaction v averaged over the two densities,

$$\text{Re } U(r) = \int d^3r_1 \int d^3r_2 \; \rho_1(r_1)\rho_2(r_2)v(r_{12}). \qquad (5)$$

(The coordinates are indicated in fig. 8.) I call this the double folding procedure.

The densities may be obtained from electron scattering studies, etc. As usual, the interaction v is an "effective" one; however, only the low density

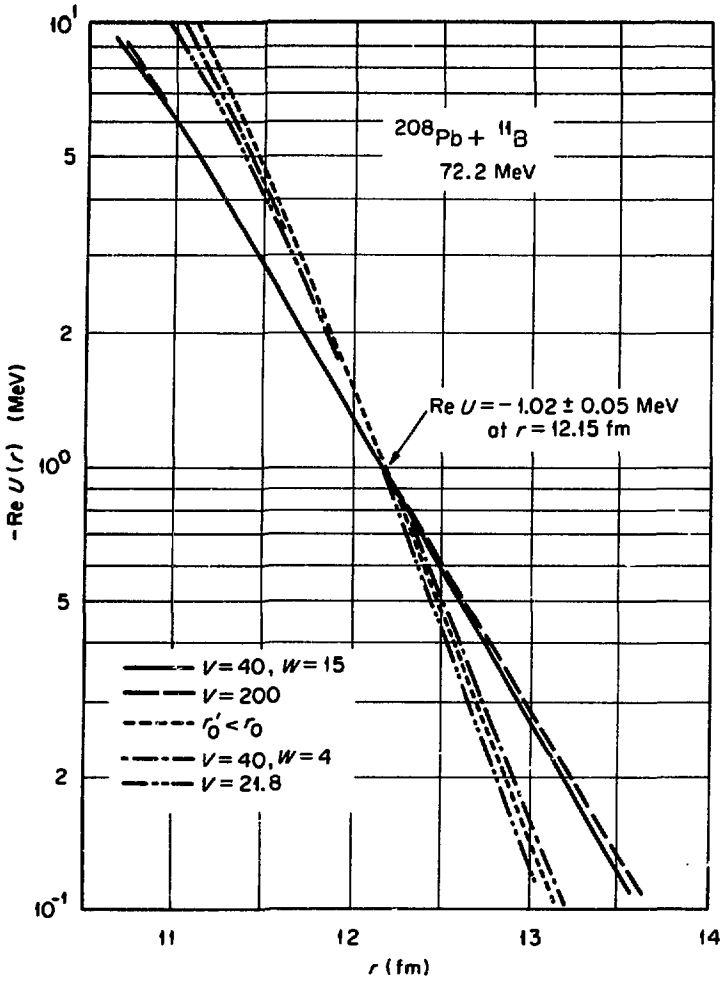

Figure 6

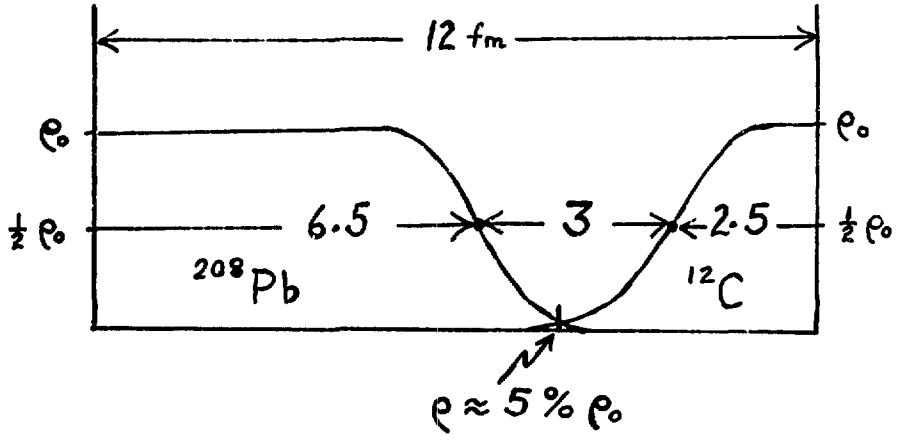

Figure 7. Densities along line of centers for $^{208}Pb+^{12}C$ for r = $D_{1/2}$.

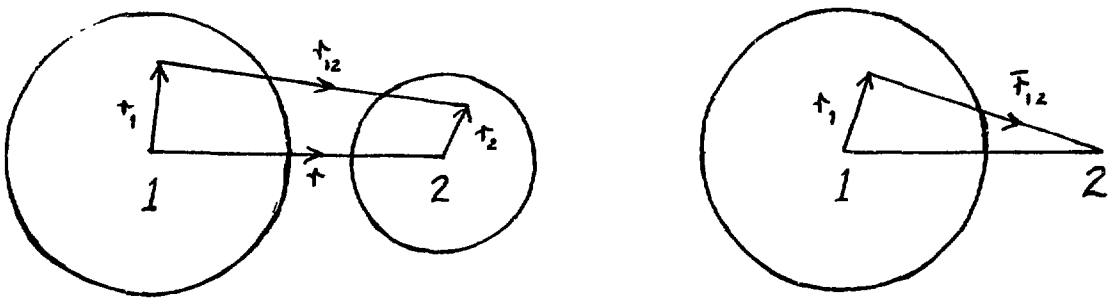

Figure 8. Left, double fold; right, single fold.

regions contribute to the integral (5) for the large separations r which are of interest, so v need not be the same as the effective interaction required for nuclear structure calculations. Indeed, one might guess that one of the simple potentials which fit low-energy nucleon-nucleon scattering would be a reasonable choice. A recent application [19] of this model has used a zero-range approximation for v so that

$$U(r) = \text{constant} \times \int \rho_1(r_1)\rho_2(|\vec{r}-\vec{r}_1|)d^3r. \tag{6}$$

These authors take the constant to be complex so that the real and imaginary parts of U have the same shape.

The finite-range form (5) has been used successfully [20] for the scattering of alphas, which shares many of the characteristics of heavy ion scattering [1].

If we consider just one of the integrations in eq. (5), we get a nucleon-nucleus potential, e.g.

$$U_{N2}(\bar{r}_{12}) = \int d^3r_2\rho_2(r_1)v(r_{12}), \tag{7}$$

so the ion-ion potential can now be written

$$\text{Re } U(r) = \int d^3r_1\rho_1(r_1)U_{N2}(\bar{r}_{12}). \tag{8}$$

(The expression (7) has been used successfully for the potential for proton scattering from nuclei [21]; however, protons are not strongly absorbed and their cross sections are not sensitive to the extreme tail of the potential but rather to its overall properties like the volume integral and mean square radius.) We may reinterpret eq. (8) by using for U_{N2} the real part of a phenomenological nucleon-nucleus optical potential determined by fitting nucleon scattering for an energy A^{-1} times the heavy ion bombarding energy [22,23]. (One should not use these prescriptions for the imaginary potential.) I call this the single folding procedure. (Of course there is an alternative procedure in which the roles of ions 1 and 2 are interchanged in eq. (8).)

Using a phenomenological nucleon potential in eq. (8) immediately implies

some energy dependence of the ion-ion potential. However, the energy dependence (or non-locality) of the latter is very much reduced compared to the former [23].

Obviously there are corrections to the prescriptions (5) or (8); e.g. McIntosh, et al. [22] considered the polarization of the density of one ion by the attractive potential of the other. However, for the present we consider how successful they are as they stand, only allowing for a renormalization in strength as a measure of higher order effects (and to compensate for our errors in choosing the effective interaction v in eq. (5)).

6. Folding and $^{12}C+^{208}Pb$

Figure 9 shows a double folded potential for $^{12}C+^{208}Pb$, using independent particle model densities and a Gaussian interaction that fits low energy nucleon-nucleon interactions [24]. To fit the data (fig. 10), it has to be multiplied by

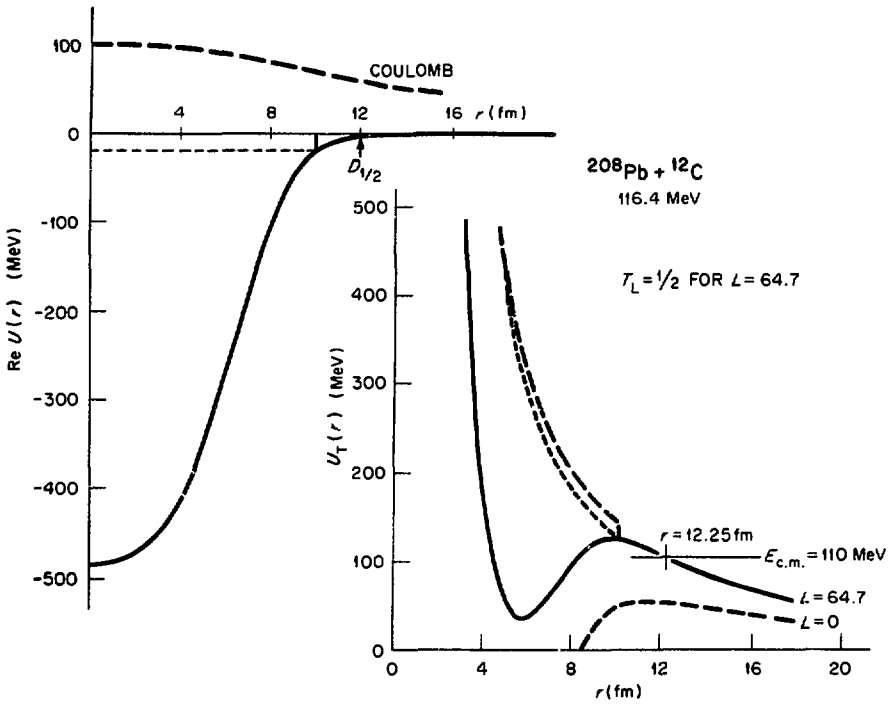

Figure 9. $U_T(r)$ is the sum of nuclear, Coulomb and centrifugal potentials.

0.59, and then has a depth of nearly 500 MeV in the interior. (This fitting was done by simply adding a W-S imaginary term with W = 15 MeV, r_o = 1.31 fm, a = 0.45 fm.) The right side of fig. 9 shows the sum of the potential plus centrifugal barrier for the (interpolated) L value for which the transmission $T_L = 1/2$. (One might expect [25] the transmission to be 50% for the energy which just equals the maximum of the barrier. However this would be true for a real barrier; the potential used here is complex and there is absorption in the barrier itself.) The turning point at 12.25 fm is very close to the turning point of the corresponding Rutherford orbit because the nuclear potential is only about 2% of the Coulomb potential here, being about 1 MeV. That is, the important part of the potential is very small compared to the interior part. To dramatize the relative importance of these two regions I cut off the real potential at 10 fm, either putting it to zero for r < 10 fm or taking it equal to -18.5 MeV, as shown in fig. 9. The effects of these two truncations are shown in fig. 10. Eliminating the potential has no effect until σ/σ_R is 1% or less, while leveling off at 18.5 MeV

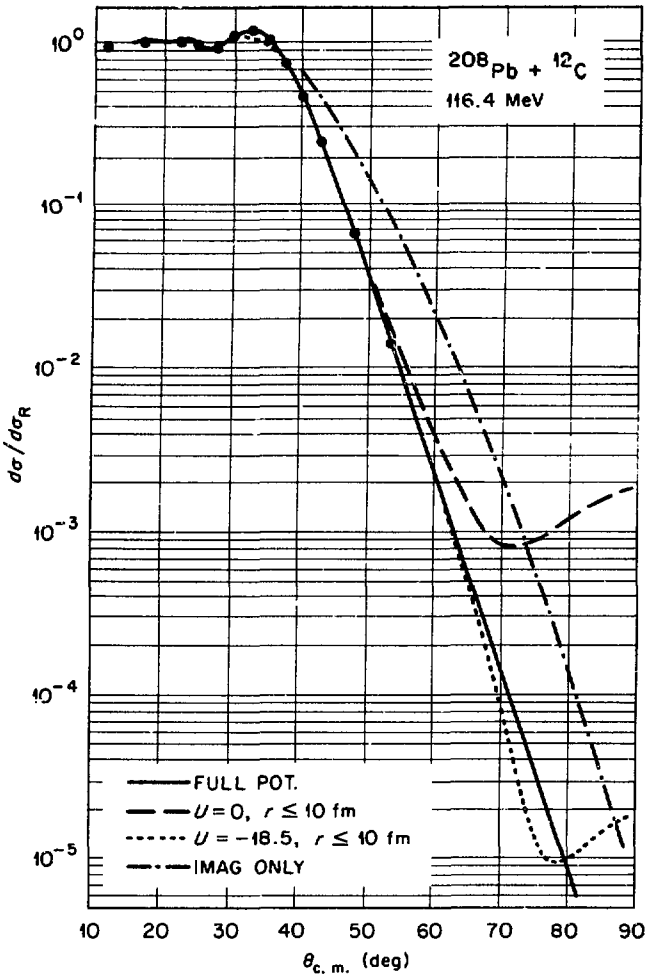

Figure 10

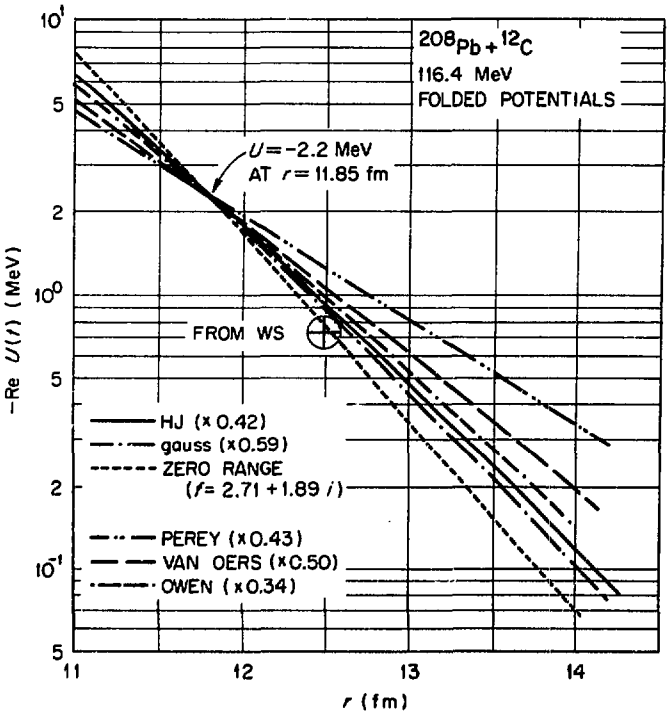

Figure 11

produces no change until $\sigma/\sigma_R < 10^{-3}$. (The abrupt change at r = 10 fm in the former case does produce some reflection.) Very similar results are obtained if the bombarding energy is raised to 200 MeV. If the absorption is reduced by reducing W from 15 to 5 MeV, the scattering becomes a little more sensitive but still very good data would be required to distinguish the cases; besides, the data definitely seems to require a larger W than this. Also shown is the scattering from the imaginary potential by itself.

Consequently it is clear one will not learn much about the potential for radii much inside the critical distance $r = D_{1/2}$, so, e.g., it is irrelevant whether or not we believe the folded potentials in the interior. Figure 11 shows various double and single fold potentials, which fit the data, near the critical radius. For the former we used also the long-range part of the Hamada-Johnston potential (HJ) and the zero-range approximation of eq. (6); the latter potential is about 1400 MeV deep for small radii. For the single folding we used 3 different choices of nucleon-^{208}Pb potential. Also shown are the renormalizing factors needed to fit the data; in each case it is necessary to reduce the predicted potential to something like one half its value. All the folded potential curves cross at $r \approx 11.85$ fm. (Curiously, various W-S potential fits to the data coincide at a slightly larger radius, as shown. I have not yet discovered the origin of this difference.)

7. Lighter Targets: $^{16}O+^{28}Si$

All the results so far have been for a heavy target. Let us turn now to $^{16}O+^{28}Si$ at 72 MeV [26], for which a fit has been obtained using a 100 MeV deep W-S potential. This potential is shown in fig. 12; the imaginary part had the

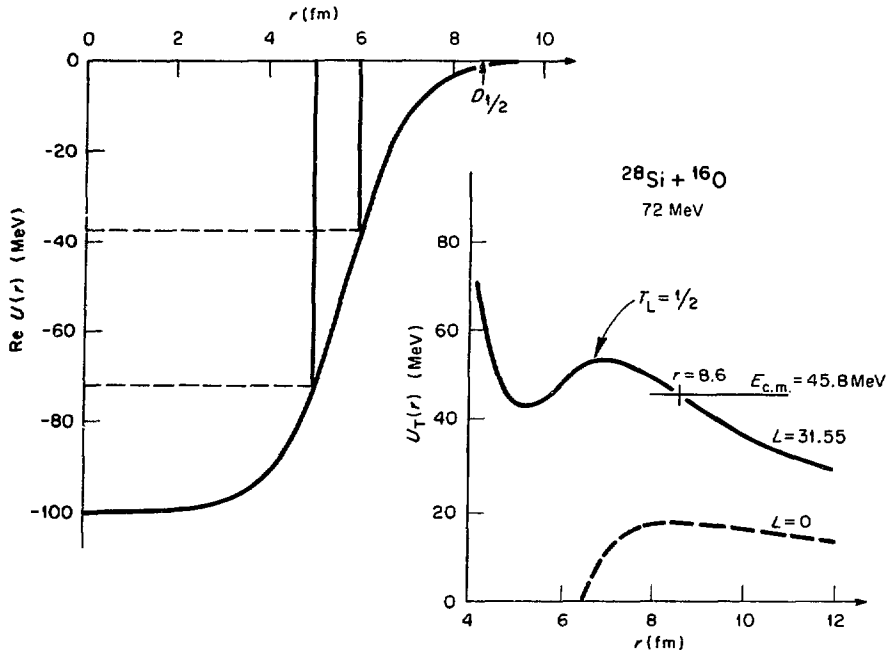

Figure 12

same shape with W = 61.5 MeV. Again the critical distance is way out in the tail and corresponds to $L \approx 31$; the potential here is about 1 MeV, still much less than the Coulomb barrier of about 20 MeV. I played the same game here; I put the whole potential (real and imaginary) equal to zero, or leveled off, for $r < 5$ fm and 6 fm. Figure 13 shows the effect on the scattering. The 6 fm cut-off does produce some effects at the $\sigma/\sigma_R \sim 10\%$ level while the cut-off at 5 fm is not felt until $\sigma/\sigma_R < 10^{-4}$. When the potential is leveled off instead of being put to zero, no noticeable effect is seen over 5 orders of magnitude in σ/σ_R. Again we see that the interior does not play an important role and its characteristics would be difficult to extract from the scattering. Further light is thrown on this by fig. 4 which shows the effect on the η_L amplitudes when the potential for $r < 6$ fm is put to zero. Only partial waves with $L < 25$ are affected and these correspond classically to Rutherford orbits which approach to $r < 7$ fm.

The ambiguity problem has been looked at by Goldberg and Smith [27] from a different point of view; they take a set of W-S wells which satisfy the Igo ambiguity and which give equally good fits to the data and consider under what conditions they could be distinguished. Figure 14 shows some results for a 200 MeV bombarding energy. A choice could be made if data were available at angles where $\sigma/\sigma_R < 10^{-2}$. They interpret the differences here in terms of differences in the rainbow scattering for the various potentials and draw a parallel with recent developments in the measurement and analysis of alpha and ^3He scattering. (However, the potentials used for fig. 14 do have the same diffuseness a; it is not clear what would happen if this constraint were relaxed. We shall see that the slope of the potential, and hence a, are not well determined by the current data.) They also study these effects as a function of energy and target mass. It is clear

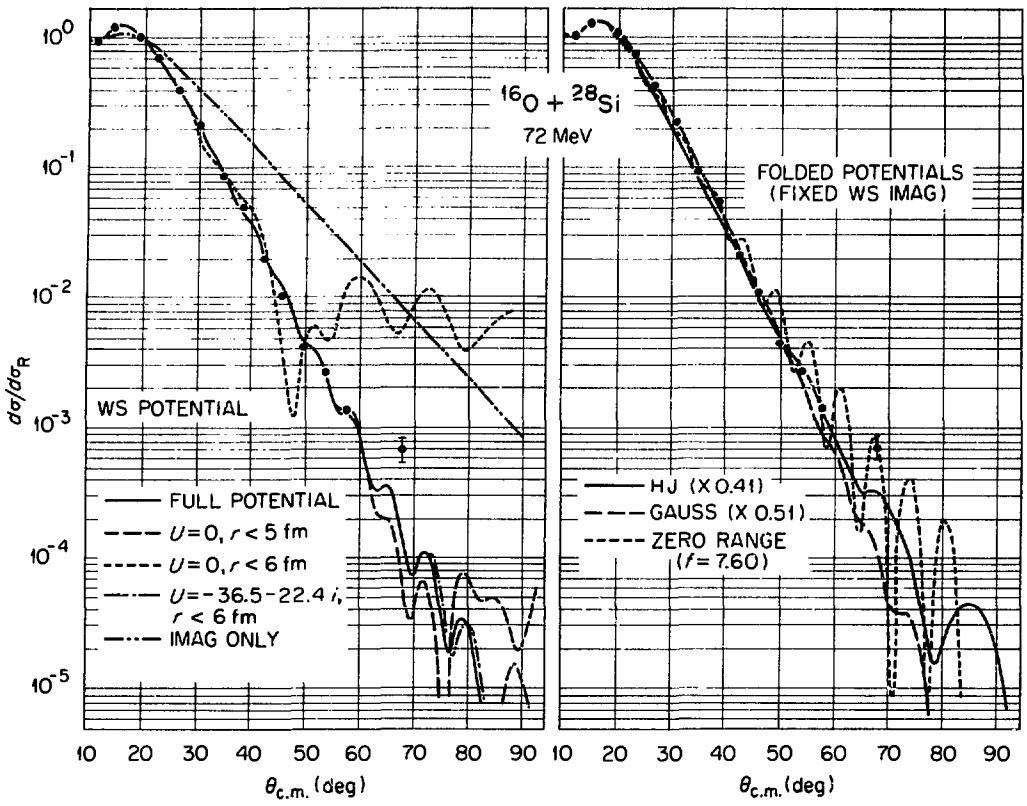

Figure 13

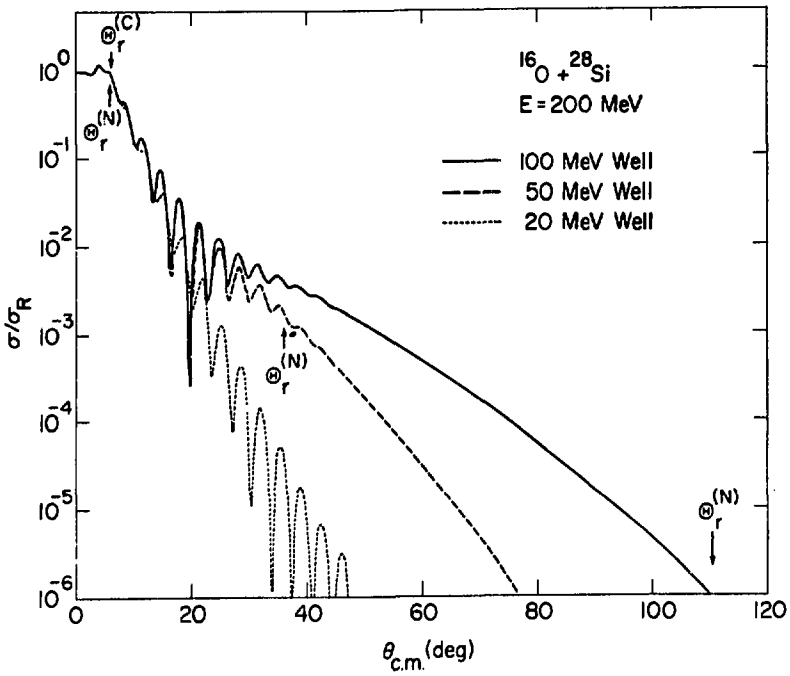

Figure 14

that the lighter the target and/or the higher the energy, the more likely is one to resolve these ambiguities.

For amusement I also reduced the absorptive potential to half the value used in fig. 13, keeping all the other parameters fixed. The predicted angular distribution (fig. 15) shows more marked oscillations than in fig. 13 but the data are fitted almost as well. This emphasizes that we have to work very hard to pin down some of these things by obtaining very complete and very precise data.

Calculations were also made for the $^{16}O+^{28}Si$ system using the double folding approach for the real potential, eq. (5). Yukawa and Gauss potentials which fit low-energy nucleon-nucleon scattering were used, as well as the long-range part of the Hamada-Johnston potential and

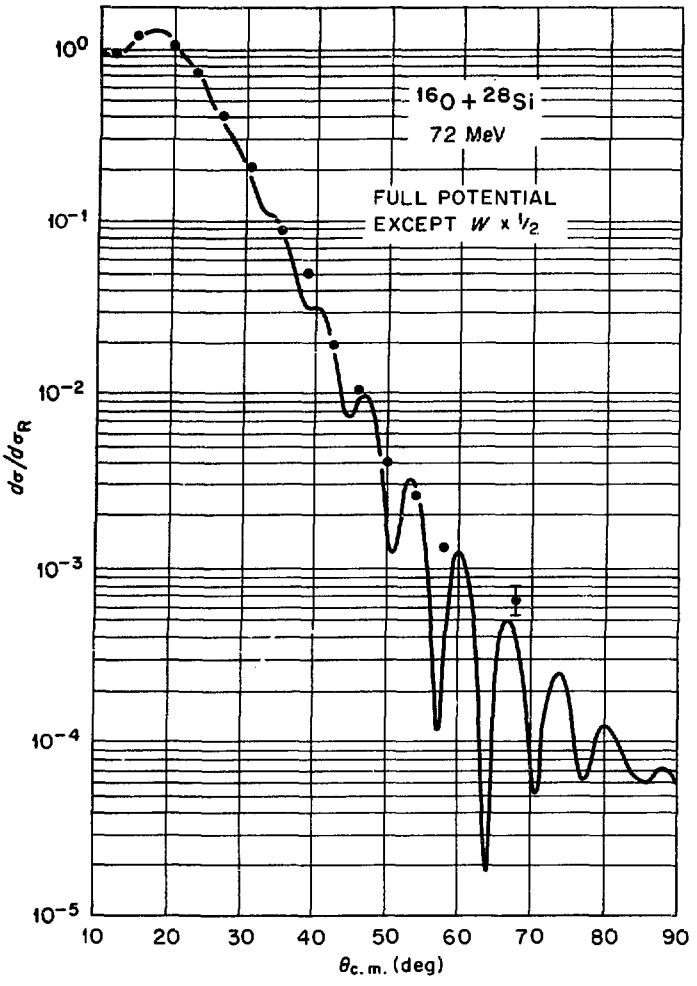

Figure 15

the zero-range approximation of eq. (6). The densities used are in accord with electron scattering measurements and were generated from the independent particle model. Some results are shown in the right half of fig. 13, for which the same W-S imaginary potential was used as before (the Yukawa results are similar). The fits to the data for the finite-range interactions are comparable to those obtained with the W-S real potential and are improved further if the imaginary potential is also adjusted. Again the predicted potential has to be reduced by one half in order to fit the data. The zero-range approximation (6) results in oscillations and a poorer fit to the data; allowing the imaginary potential strength to vary or giving it the same shape as the real did not remove these oscillations.

The corresponding real potentials near the critical radius are shown in fig. 16. They cross just inside $r = D_{1/2}$, except for the zero-range potential which is steeper than the others. The values of U(r) at r = 0 are also shown; the zero-range potential (with f = 7.6 MeV fm^3) is extremely deep.

These ambiguities persist for even lighter targets. I have not explored this region much, but fig. 17 shows an example for 168 MeV ^{16}O on ^{12}C [28]. The solid curve is a 4-parameter W-S potential fit obtained by Bassel [29]; it is a relatively shallow potential (V = 30.6 MeV, W = 17.2 MeV, R = 5.64 fm, a = 0.65 fm). Now Charles, et al. [22] had found that a single-folded potential could reproduce the main features of $^{16}O+^{12}C$ scattering at 24, 42 and 51 MeV over the whole angular range up to 170°. I used their folding model parameters, with Bassel's W-S imaginary potential unchanged, to produce the curve labelled "fold" in fig. 17; the real potential was reduced in strength by 20% to improve the fit to the data. The fit is seen to be comparable in quality and could be improved further by readjusting the imaginary potential. This folded potential is 380 MeV deep in the interior but coincides with Bassel's W-S potential for radii beyond 6 fm. Already by 5 fm the folding gives twice as strong a potential, so the scattering in this case will not tell us much about the potential at distances less than 6 fm.

8. Inelastic Scattering

Many of the remarks made about elastic scattering also have analogues for inelastic scattering. In particular, a study of the interference between Coulomb and nuclear excitation gives a sensitive measure of the transition potential at

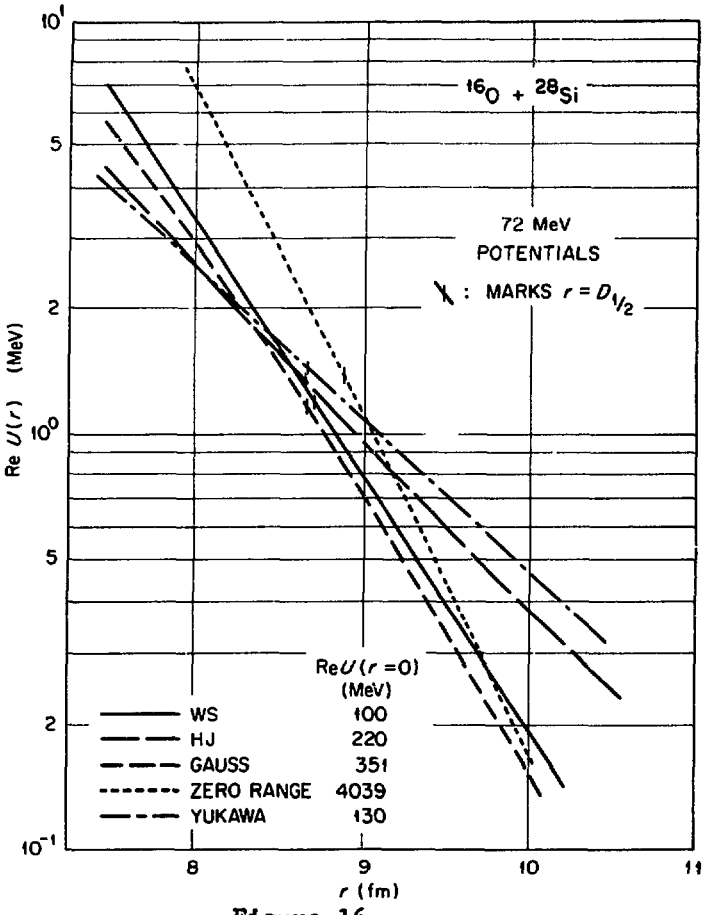

Figure 16

some large radius which is similar to, but not necessarily the same as, the critical radius determined from elastic data [4]. In order to relate this to the optical potential one has to assume some relationship between the diagonal elastic potential and the off-diagonal transition potential. This is usually done through the collective model by simply deforming the optical potential [4]. However it must be recognized that this is an additional assumption. An attractive possibility is that an approach analogous to the double folding (5) would work and in that way a unified description could be obtained. The transition densities could be obtained phenomenologically or microscopically from nuclear wavefunctions. The latter approach has had some success with proton scattering [30]. Alternatively the single fold procedure might be used. At least one application of the latter has been made to heavy ion scattering [31]. The emphasis on large separations in heavy ion reactions may mean that exchange effects are less important than for light ions [32].

9. Concluding Remarks

We have seen that a characteristic of heavy ion scattering is to determine the value of the real part of the ion-ion potential at a critical radius of separation which is close to the distance of closest approach $D_{1/2}$ for the Rutherford orbit which has a transmission coefficient $T_L = 1/2$. It is the value at this point, not the slope (or surface diffuseness a), which is well determined, at least in the cases I have looked at. Within this context it would be good if authors making optical model analyses would quote the values of these physically significant quantities $L_{1/2}$, $D_{1/2}$ and $ReU(r = D_{1/2})$.

A more complete picture of the ion-ion potential (although still only of its surface aspects) is obtained by studying other peripheral events like inelastic scattering and transfer reactions. With the sorts of energies currently available (say $\lesssim$ 10 MeV/nucleon) it is difficult to obtain more detailed information from elastic scattering. The data for heavy targets are dominated by the Coulomb effects. Light nuclei minimize these but then one encounters strong-coupling fluctuations [33], exchange processes and other special structural features. Intermediate nuclei, such as the s,d shell and perhaps p,f shell nuclei would seem to be the most favourable targets at present. Even then one has to work hard by measuring small cross sections at small enough angular intervals that the distributions are well defined. At that point one has to worry that inelastic scattering to some particular state has become strong enough that its effects have to

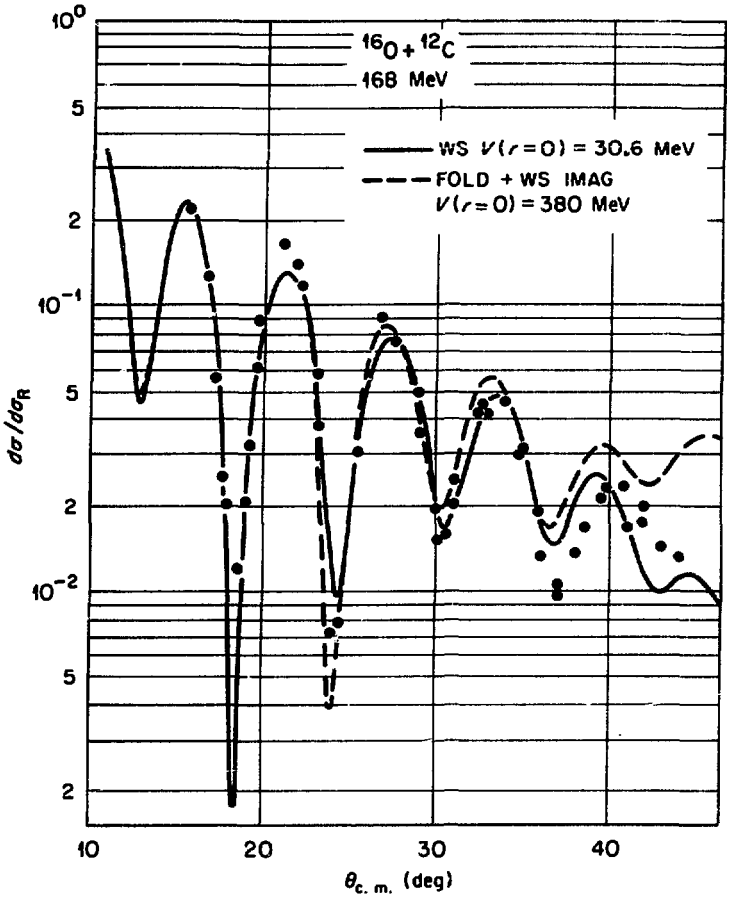

Figure 17

be taken into account explicitly rather than being included in an average way in the usual simple potential model. (Of course that particular worry is not experimental but is simply concerned with the complexity of the theoretical analysis required.)

The important interaction region is where the ion densities are very low, so one is encouraged to explore simple models of the real potential such as the folding procedures of eqs. (5) and (8). These give very deep potentials in the interior, several 100 MeV, but this is no drawback since these are not experienced by the scattering process. They give one the hope of relating the ion-ion potential to other quantities such as the nucleon-nucleus optical potential or nucleon-nucleon effective interactions. (However, one should not expect these procedures to work, except by "accident", for the imaginary potential.)

For the examples examined here, as well as some $^{16}O+^{208}Pb$ calculations I have done, the simple folded potentials need renormalizing to roughly half their predicted values in order to fit the data. (The results of Brink and Rowley [22] seem to support this conclusion. They adjust U_{N2} of eq. (8) to fit the heavy ion elastic data; the U_{N2} they obtain are smaller than might be expected from nucleon scattering data and this is consistent with my need for renormalization. In addition the densities they use have rather small radii; larger radii would decrease their U_{N2} even further.) The reason for the renormalization is not understood at present. I believe exchange effects are small but in any case would tend to make the discrepancy larger. Distortion of the surface density of one ion in the field of the other has been neglected; the effect of the attractive nuclear field [22] is to increase the density and hence the potential, but the much larger repulsive Coulomb field would reduce it. Estimates of this effect are being made.

The zero-range form (6) gives very deep potentials. For example, a relatively light projectile of mass A on a heavy target results in $U(r=0) \approx 40\ A\ \bar{f}$ MeV, where $\bar{f}$ is the strength parameter of Vary and Dover [19]. Typically $Re\bar{f} \approx 5$ so $ReU(r=0) \approx 200\ A$ MeV or ~ 3000 MeV for an ^{16}O projectile. More importantly it may give a more rapid decay of U(r) in the tail region than does folding with a finite range interaction. Its decay length is about the same as one obtains with the Gaussian potential [24], but appreciably smaller than with Yukawa-type potentials which include a range like the OPEP. Fits to scattering data for heavy targets (including $^{16}O+^{208}Pb$ at 192 MeV) and 60 MeV ^{16}O on medium weight targets [19] can be obtained which are as good as those using finite range interactions, but the scattering of 72 MeV ^{16}O from ^{28}Si is appreciably different (fig. 13).

References

(The references chosen are intended to be representative rather than comprehensive.)

[1] J. S. Blair, in Proc. conf. on nuclear reactions induced by heavy ions, ed. W. Hering and R. Bock (North-Holland, Amsterdam, 1970).

[2] W. E. Frahn, Ann. Phys. (N.Y.) 72 (1972) 524;
R. A. Broglia and A. Winther, Phys. Reports 4C (1972) 153.

[3] B. Nilsson, R. A. Broglia, S. Landowne, R. Liotta and A. Winther, Phys. Lett. 47B (1973) 189;
M. C. Lemaire, M. C. Mermaz, H. Sztark and A. Cunsolo, Phys. Rev. C, to be published.

[4] P. R. Christensen, I. Chernov, E. E. Gross, R. Stokstad and F. Videbaek, Nucl. Phys. A207 (1973) 433.

[5] M. C. Bertin, S. L. Tabor, B. A. Watson, Y. Eisen and G. Goldring, Nucl. Phys. A167 (1971) 216;
B. C. Robertson, J. T. Sample, D. R. Goosman, K. Nagatani and K. W. Jones, Phys. Rev. C4 (1971) 2176;
A. M. Friedman, R. H. Siemssen and J. G. Cuninghame, Phys. Rev. C6 (1972) 2219;
H. H. Gutbrod, M. Blann and W. G. Winn, Nucl. Phys. A213 (1973) 285.

[6] W. E. Frahn and R. H. Venter, Ann. Phys. (N.Y.) 24 (1963) 243;
R. Anni and L. Taffara, Riv. Nuovo Cimento 2 (1970) 1.

[7] P. R. Christensen, V. I. Manko, F. D. Becchetti and R. J. Nickles, Nucl. Phys. A207 (1973) 33 and A203 (1973) 1.

[8] K. W. McVoy, Phys. Rev. C3 (1971) 1104;
R. C. Fuller, Nucl. Phys. A216 (1973) 199;
R. C. Fuller and Y. Avishai, Nucl. Phys. A222 (1974) 365;
R. C. Fuller and O. Dragun, to be published.

[9] G. H. Rawitscher, Nucl. Phys. 85 (1966) 337.

[10] U. Mosel, T. D. Thomas and P. Reisenfeldt, Phys. Lett. 33B (1970) 565;
W. Scheid and W. Greiner, Z. Physik 226 (1970) 364.

[11] U. Mosel, Particles & Nuclei 3 (1972) 297;
P. Lichtner, D. Drechsel, F. Maniler and W. Greiner, Phys. Rev. Lett. 28 (1972) 829.

[12] G. Helling, W. Scheid and W. Greiner, Phys. Lett. 36B (1971) 64.

[13] P. Schumacher, N. Ueta, H. H. Duhm, K. I. Kubo and W. J. Klages, Nucl. Phys. A212 (1973) 573.

[14] R. A. Chatwin, J. S. Eck, D. Robson and A. Richter, Phys. Rev. C1 (1970) 795;
D. Robson, in Heavy ion scattering, Argonne National Laboratory Report ANL-7837 (1971).

[15] J. Orloff and W. W. Daehnick, Phys. Rev. C3 (1971) 430.

[16] J. L. C. Ford, Jr., K. S. Toth, D. C. Hensley, R. M. Gaedke, P. J. Riley and S. T. Thornton, Phys. Rev. C8 (1973) 1912.

[17] J. L. C. Ford, Jr., K. S. Toth, G. R. Satchler, D. C. Hensley, L. W. Owen, R. M. DeVries, R. M. Gaedke, P. J. Riley and S. T. Thornton, Phys. Rev. C, to be published.

[18] Y. Eisen, Phys. Lett. 37B (1971) 33.

[19] J. P. Vary and C. B. Dover, Phys. Rev. Lett. 31 (1973) 1510.

[20] C. J. Batty, E. Friedman and D. F. Jackson, Nucl. Phys. A175 (1971) 1; A. Budzanowski, A. Dudek, K. Grotowski, Z. Majka and A. Strzalkowski, Particles & Nuclei 6 (1973) 97.

[21] D. Slanina and H. McManus, Nucl. Phys. A116 (1968) 271; G. W. Greenlees, W. Makofsky and G. J. Pyle, Phys. Rev. C1 (1970) 1115.

[22] J. S. McIntosh, S. C. Park and G. H. Rawitscher, Phys. Rev. 134 (1964) B1010; P. Charles, M. Dost, B. Fernandez and J. Gastebois, in CEN Saclay annual report (1972); L. West, S. Cotanch and D. Robson, contribution to Munich Conference (1973); D. M. Brink and N. Rowley, Nucl. Phys. A219 (1974) 79.

[23] D. F. Jackson and R. C. Johnson, Phys. Lett. 49B (1974) 249.

[24] I. Reichstein and Y. C. Tang, Nucl. Phys. A139 (1969) 144.

[25] K. W. Ford, D. L. Hill, M. Wakano and J. A. Wheeler, Ann. Phys. (N.Y.) 7 (1959) 239.

[26] J. G. Cramer, R. M. DeVries, M. S. Zisman, K. G. Nair, K. L. Liu and Y. D. Chan, contribution to Munich Conference (1973).

[27] D. A. Goldberg and S. M. Smith, Phys. Rev. Lett. 29 (1972) 500 and to be published.

[28] J. C. Heibert and G. T. Garvey, Phys. Rev. 135 (1964) B346.

[29] R. H. Bassel, G. R. Satchler and R. M. Drisko, Nucl. Phys. 89 (1966) 419.

[30] G. R. Satchler, Comments on Nucl. & Part. Phys. 5 (1972) 39; Z. Physik 260 (1973) 209.

[31] L. West, S. Cotanch and D. Robson, contribution to Munich Conference (1973).

[32] G. R. Satchler, Phys. Lett. 39B (1972) 495.

[33] H. J. Fink, W. Scheid and W. Greiner, Nucl. Phys. A188 (1972) 259.